Achievable Capacity of Cognitive Radio Systems Coexisting with a Macro Cellular System

Hiromasa Fujii, Shunji Miura and Hidetoshi Kayama

Research Laboratories, NTT DOCOMO, Inc.
3-6 Hikari-no-oka, Yokosuka, Kanagawa, Japan
Email: {fujiihir, miurasy, kayama}@nttdocomo.co.jp

***Abstract*—A theoretical analysis of achievable capacity by a cognitive radio systems is discussed, when the cognitive radio system (CRS) uses spectrum allocated to a macro cellular system. As for the spectrum sharing mechanisms, we consider two methods based on listen-before-talk and adaptive transmit power control principles. Moreover, outdoor and indoor installations of CRS stations are investigated. Numerical results reveal capacities achieved by CRS base stations installed within the coverage area of the macro cell system.**

I. Introduction

Spectrum sharing remains one of the most important goals for wireless communication systems. Up until recently, the principle has been to assign exclusive frequency bands to different systems or different operators (exclusive usage), and systems that used adjacent frequency channels were required to use appropriate spectrum masks to avoid harmful interference with each other. Recent wireless communication systems such as 3GPP LTE [1] and future 4G systems including IMT-Advanced [2] require wide frequency bands to enable high speed data transmission, although it is extremely difficult to allocate new spectrum resources due to the scarcity of newly allocatable frequencies.

To tackle this problem, one challenging approach is to completely overlap the occupied frequency bands of several systems using cognitive radio techniques [3], [4], [5]. In this case, each terminal of cognitive radio systems (CRSs) has to recognize its ambient conditions and judge whether or not it can start sending signals without harmful interference to the prioritized systems. A lot of radio application services such as land-mobile, satellite, radar, broadcasting, are currently in services, then a lot of possible scenario can be considered for the spectrum sharing. Here, we focus on spectrum sharing between a macro cellular system (MCS) and CRS.

Analytical capacity of a spectrum sharing environment has been already studied in many literatures e.g. [6], [7], [8] from variery of viewpoints about sharing mechanizms, policies, scenario and so on. Here we focus on [6], where average capacities of CRS are derived under the following assumption: (i) victim receivers distributes uniformly around the CRS stations, (ii) sharing mechanizms works ideally, (iii) CRS system is so-called point-to-multipoint wireless network. However, [6] assumes a spectrum sharing scenario where the interfering signal from the prioritized system to CRS receiver is negligible. Moreover, [6] do not take wall losses into account, since all CRS stations are assumed to be located out of doors and the study assumes proportional fair scheduling, which is not appropriate for the spectrum sharing between MCSs and CRSs. In such a spectrum sharing scenario, a lot of victim receivers, MCS mobile stations (MSs), will be located around CRS stations in this sharing scenario. Then CRS systems must not be able to transmit large signal during large portion of the time, which indicates the deployment scenario of CRS in this case may be limited to the hotspot service. Thus, the number of active terminals simultaneously connecting to a CRS base stations (BSs) is quite a few and the channels between CRS BS and MS should be quasi-static, where assumption of proportional fair may overestimate achievable capacity of CRS systems.

In this paper, we drive analytical the capacity achieved by a CRS when the CRS and an MCS share a spectrum band. The analysis is based on the study [6] and the same underlying assumption is that CRS does not give harmful interference to the MCS. As for the spectrum sharing mechanisms, two methods are considered; one is based on listen-before-talk (LBT) principle and the other is the method utilizing adaptive transmit power control (ATPC) [6]. We also investigate the indoor and outdoor scenarios for the installation of CRS BSs and assume round robin scheduler for CRS BSs.

The remainder of this paper is as follows: Section II explains assumed spectrum sharing environment and a sharing mechanism. Next, in section III we derive the analytical capacity achieved by CRSs coexisting with an MCS. Lastly, we show numerical results and performance comparisons in Section IV, which is followed by our conclusions in Section V.

II. Spectrum sharing environment and a sharing mechanism

Fig. 1 shows an assumed spectrum sharing environment. Here an MCS and a CRS share a spectrum band, where the MCS have priority over the CRS for the spectrum usage. In this study we focus on the downlink transmission of the CRS. Then MCS MSs are victim receivers to be secured from harmful interference and MCS BSs are the interfering source to the CRS.

Two sharing mechanisms are considered: one is based on Listen Before Talk principle and the other applies adaptive transmit power control [6]. LBT method allows CRS stations to transmit signals with the predetermined transmit power only if the transmitted signal does not give harmful interference to the MCS stations. Then, each CRS stations sense the signals from MCS MSs and if the observed signal levels are

CROWNCOM 2011, June 01-03, Osaka, Japan

DOI 10.4108/icst.crowncom.2011.245822

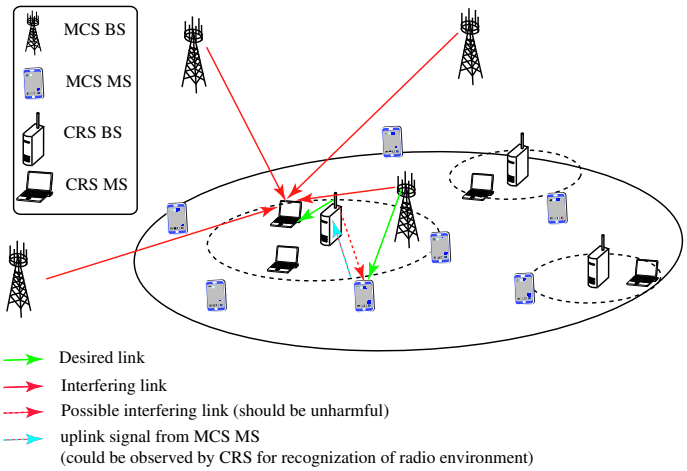

Fig. 1. Spectrum sharing environment

above predetermined threshold, CRS stations transmit signals; otherwise they refrain to send signals. On the other hand, ATPC method allows CRS stations send signals with the transmit power $P_{allow,crs}$ [dBm], which secures interference power under allowable level $I_{allow,mcs}$ at all MCS MSs. Thus the MCS MS interfered mostly by the CRS BS should be cared for. To obtain $P_{allow,crs}$, the path loss L_{path} [dB] between the MCS MS and the CRS station have to be estimated by observing uplink signals form MCS MSs at the CRS BS, for example.

$$L_{path} = R_{crs,bs} - \left(P_{tx,mcs,ms} + G_{mcs,ms} + G_{crs,bs}\right) \quad (1)$$

where $R_{crs,bs}$ [dBm] is received signal power from the MCS MS and the CRS BS, and $P_{tx,mcs,ms}$ is the transmit power of MCS MSs. $G_{mcs,ms}$ [dBi] and $G_{crs,bs}$ [dBi] are the antenna gain of MCS MS and CRS BS Moreover, to calculate $P_{allow,crs}$, allowable interference level at MCS BS $I_{allow,mcs}$ [dBm/Hz] is known at the CRS BS.

$$P_{allow,crs} = G_{crs,bs} - L_{path} + G_{mcs,ms} + I_{allow,mcs} + BW_{crs} \quad (2)$$

where BW_{crs} [dBHz] is the occupied bandwidth of the CRS.

Lastly, we consider two conditions for the locations of CRS terminals, which are indoor and outdoor, while MCS stations reside outside of the buildings. For the cases when CRS stations are located in indoor sites, penetration losses by building outer walls are taken into consideration for the following two kinds of paths (see Fig. 2):

1) path from a CRS BS to an MCS MS
2) path from an MCS BS to a CRS MS

III. Capacity analysis of CRS coexisting with an MCS

In this section, we derives the attainable capacity of a CRS when the CRS coexisting with an MCS based on the analysis shown in [6]. Firstly, we explain how to calculate average cell capacity for given transmit power in the section III.A, and next the section III.B show how to calculate probability of allowable transmit power and capacity of a CRS coexisting with an MCS.

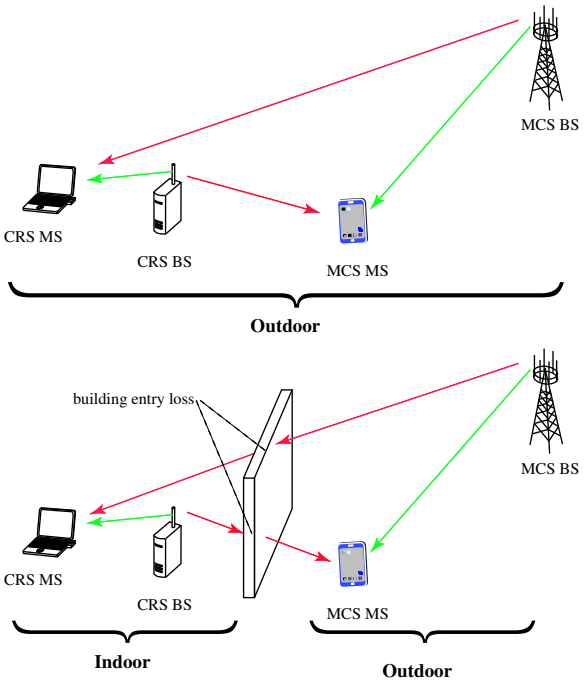

Fig. 2. Indoor and outdoor scenario of the CRS station locations

A. Average cell capacity for given transmit power

When transmit power of a CRS BSis $P_{tx,crs}$ [dBm], the average cell capacity over area A is obtained by

$$C_{cell}(P_{tx,crs}) \text{ [bps/Hz]} = \frac{1}{S_A} \times \int_A \int_{-\infty}^{\infty} C_k(Z(P_{tx,crs})) p_{sh}(v_{sf}, m_{sh}) \, \mathrm{d}v_{sf} \, \mathrm{d}a \quad (3)$$

where $Z(P_{tx,crs})$ [dB] is the signal to interference and noise ratio (SINR), S_A is cell size, v_{sf} is a shadowing factor, and $p_{sh}(v_{sf}, m_{sh})$ is the PDF of v_{sf} with variance σ^2.

$$p_{sh}(v_{sf}, m_{sh}) = \frac{1}{\sqrt{2\pi\sigma^2}} e^{-\frac{(v_{sf}-m_{sh})^2}{2\sigma^2}} \quad (4)$$

where m_{sh} is determined using the following equation (5) so as not to change the mean path losses by introducing the shadowing effects.

$$m_{sh} = -10 \times \log_{10} \int_{-\infty}^{\infty} 10^{v_{sf}/10} p_{sh}(v_{sf}, 0) \mathrm{d}v_{sf} \quad (5)$$

$Z(P_{tx,crs})$, which is denoted Z by omitting $P_{tx,crs}$ below, is calculated as

$$Z = 10^{P_{tx,crs} + G_{crs,bs} - BW_{crs} - L_{path} + v_{sf} + G_{crs,ms} - P_{IN}} \quad (6)$$

where P_{IN} [dBm/Hz] is the interference plus noise power density at the receiver. P_{IN} is calculated from thermal noise density $N_{thermal}$ [dBm/Hz] and the noise figure NF [dB] and interfering signal power density P_I [dBm/Hz].

$$P_{IN} = 10 \times \log_{10} \left(10^{(N_{thermal} + NF)/10} + P_I\right) \quad (7)$$

TABLE I
SYSTEM PARAMETERS

Common parameters	
frequency	2 GHz
$N_{thermal}$	-174 dBm/Hz
σ	4 dB
C_{comp}	8 dB
C_{max}	7 bps/Hz
L_{wall}	20 dB
M_{IN}	-10 dB
MCS parameters	
$P_{tx,mcs}$	43 dBm
BW_{mcs}	20 MHz
$G_{mcs,bs}$	17 dBi
$G_{mcs,ms}$	0 dBi
NF	6 dB
BS antenna height	30 m
MS antenna height	1.5 m
$p_{active,mcs}$	0.1
CRS parameters	
$P_{tx,crs,max}$	20 dBm
BW_{crs}	20 MHz
$G_{crs,bs}$	5 dBi
$G_{crs,ms}$	0 dBi
NF	6 dB
BS antenna height(outdoor)	10 m
BS antenna height(indoor)	3 m
MS antenna height	1.5 m
$d_{cr,target}$	30 m

TABLE II
APPLIED PROPAGATION MODELS

MCS BS - MCS/CRS MS	COST-231 HATA[9]	
CRS BS - CRS BS - MCS/CRS MS	outdoor	M2135 (Micro urban, hexagonal cell layout) [10]
	indoor	M2135 (Indoor hotspot, NLOS) [10]

Moreover, P_I is obtained as a total signal power from all the MCS BS and then the P_I becomes

$$P_I = \sum_{i \in S_{mcs,bs}} 10^{P_{tx,mcs}+G_{mcs,bs}-BW_{mcs}-L_{path,i}+G_{crs,ms}} \quad (8)$$

where $S_{mcs,bs}$ is the set of MCS BSs and $L_{path,i}$ is the path loss between MCS BS i and the CRS MS, $P_{tx,mcs}$ and $G_{mcs,bs}$ is the antenna gain of MCS BS. BW_{mcs} is the system bandwidth of MCS. We regard the interference level at CRS MSs as those of their serving CRS BS, for simplicity

Lastly, the relation between capacity $C(Z)$ [bps/Hz] and SINR Z is obtained by

$$C(Z) = \log_2(1 + Z/C_{cmp}), \quad (9)$$

where C_{cmp} is a compensation factor that depends on system capabilities.

B. Capacity of CRS coexisting with an MCS

In the spectrum sharing environment, the received interference power at MCS MSs should be below the acceptable interference level $I_{allow,mcs}$ [dBm/Hz],

$$\begin{aligned} I_{allow,mcs} \quad > \quad & P_{tx,crs} - BW_{crs} + G_{crs,bs} \\ & - L_{path} + G_{mcs,ms} \end{aligned} \quad (10)$$

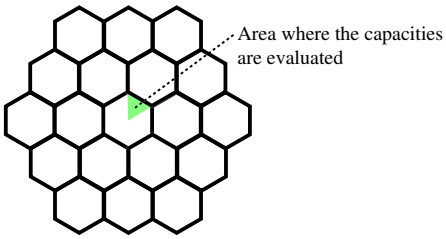

Fig. 3. Cell structure of the MCS

Next, the condition defines interfering distance d_{ia}. We model path losses as:

$$L_{path} = \alpha \log_{10}(d) + \beta \quad (11)$$

where d is the distance between a transmitter and a receiver. If the path goes across the wall between indoor and outdoor sites, an additional wall loss L_{wall} is considered. α and β are constants which depends on the radio channel conditions including the frequency and the antenna heights. Based on the above assumptions, d_{ia} [m] becomes

$$d_{ia} = 10^{\frac{P_{tx,crs}+\gamma-\beta}{\alpha}} \quad (12)$$

where

$$\gamma = G_{crs,bs} + G_{mcs,ms} - BW_{crs} - I_{allow,mcs}. \quad (13)$$

Here we omit effects of shadowing and multipath fading in determining d_{ia}.

If MCS MSs are distributed uniformly over the area, the number of MCS MSs in the interfering area, $N_{mcs,ms}$ is

$$N_{mcs,ms} = \rho_{mcs,ms} \pi d_{ia}^2 \quad (14)$$

where $\rho_{mcs,ms}$ [terminals/m^2] is the density of the MCS MSs whose packet are in the queue of downlink schedulers. Using $N_{mcs,ms}$, we can obtaind the probability with which the CRS BS can transmit signal with the power $P_{tx,crs}$.

$$F_{txp}(P_{tx,crs}) = (1 - p_{active,mcs})^{N_{mcs,ms}} \quad (15)$$

where $p_{active,mcs}$ is the probability that an MCS MS is active, which means the MCS MS is receiving data.

Finally, the cell-averaged capacity achieved by LBT is given as follows:

$$C_{cell,LBT}(P_{tx,crs})\,[\text{bps/Hz}] = C_{cell}(P_{tx,crs}) F_{txp}(P_{tx,crs}) \quad (16)$$

As for the ATPC case, the capacity becomes

$$\begin{aligned} & C_{cell,ATPC}\,[\text{bps/Hz}] = \\ & \int_0^{\infty} C_{cell}(\min(P_{tx,crs}, P_{tx,crs,max})) f_{txp}(P_{tx,crs}) \quad \mathrm{d}P_{tx,crs} \end{aligned} \quad (17)$$

where $P_{tx,crs,max}$ [dBm] is maximum transmit power of the CRS BS and $f_{txp}(P_{tx,crs})$ is the probability that the CRS BS transmits at P_{tx} with the ATPC, which is obtained by differentiating $F_{txp}(P_{tx})$ as follows:

$$\begin{aligned} f_{txp}(P_{tx,crs}) \quad = \quad & -F(P_{tx,crs}) \ln(1 - p_{active,mcs}) \\ \times \quad & \rho_{mcs,ms} \pi \frac{2}{\alpha} \ln(10) 10^{2\frac{P_{tx,crs}+\gamma-\beta}{\alpha}} \end{aligned} \quad (18)$$

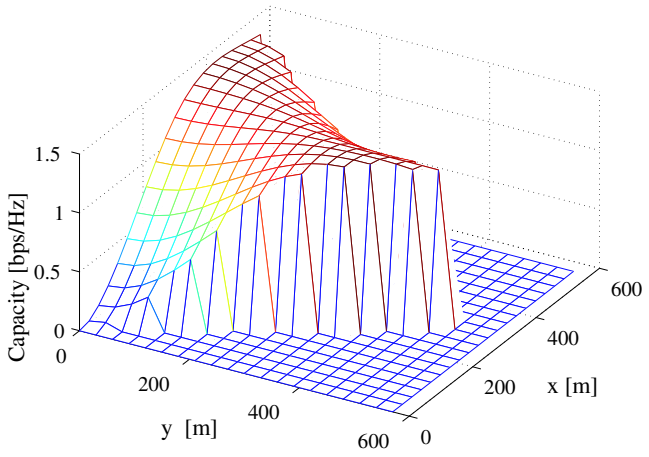

Fig. 4. Achievable capacity by the CRS with ATPC, outdoor, $\rho_{mcs,ms}$ =2 $\times 10^{-4}$ user/m^2

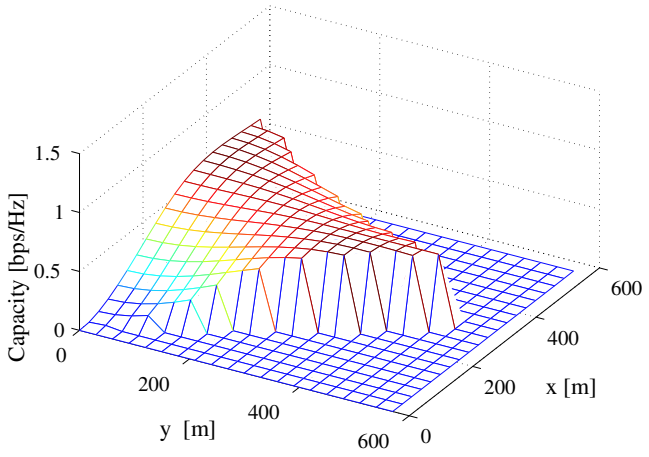

Fig. 5. Achievable capacity by the CRS with LBT ($P_{tx,crs} = 10$ dBm), outdoor, $\rho_{mcs,ms}$=2 $\times 10^{-4}$ user/m^2

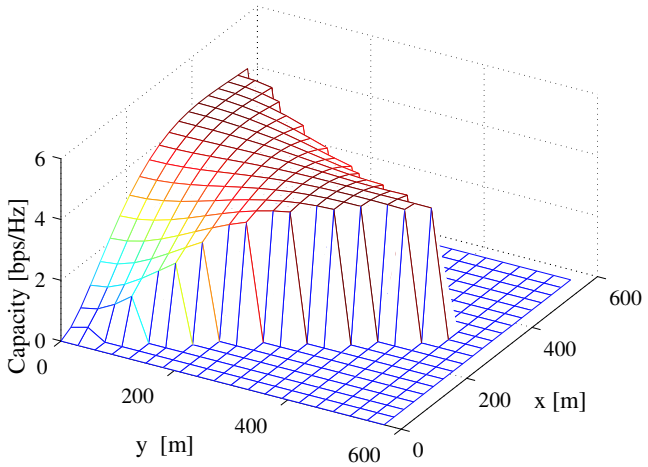

Fig. 6. Achievable capacity by the CRS with ATPC, indoor, $\rho_{mcs,ms}$=2 $\times 10^{-4}$ user/m^2

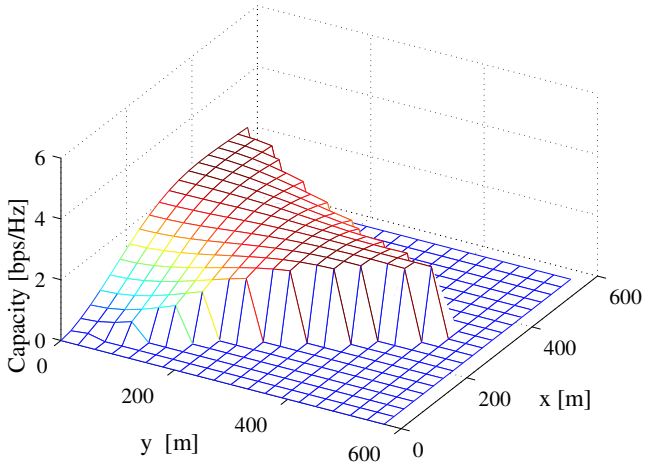

Fig. 7. Achievable capacity by the CRS with LBT ($P_{tx,crs} = 10$ dBm), indoor, $\rho_{mcs,ms}$=2 $\times 10^{-4}$ user/m^2

IV. Numerical results & performance comparisons

Table II shows the parameters used for the numerical results. Table II shows the path loss models applied to obtaine the numerical results and additional wall penetration loss is considered if required. 19-cell structure is assumed for the deployment of MCS BSs and CRS BSs are located in covered area of the center cell as shown in Fig 3. On the calculation of the capacity, only a triangle area in the cell area is counted considering the symmetrical feature. We also assume omni-directional antennas are assumed for all stations.

Fig. 4 shows geographical distribution of achievable capacity by the CRSs when ATPC is applied for the sharing mechanism. $P_{tx,crs}$ in LBT cases is set to 10dBm, which is common in the following three results. CRS BSs and CRS MSs are located in outdoor. In this figure, a value at a location specified by x and y means the averaged capacity obtained by a CRS BS when the CRS BS is installed at the point. The result shows the capacities are quite small if the CRS BS is located close to an MCS BS and capacity becomes large as the CRS BS location goes off MCS BSs. This is simply because the signal power from MCS BSs is strong at the vicinity of an MCS BS, which is interference for the CRS MS. Thus SINR at the CRS MS deteriorates, which result in small capacity in the area.

Fig. 5 shows geographical distribution of achievable capacities by CRS BSs, when LBT is used. CRS stations are installed outdoor area. The tendency of the capacity distribution is the same with the ATPC case, however, the overall capacities are far smaller than those of the ATPC case. This is because LBT does not utilize path lose information between CRS BSs and MCS MSs, thus lose potential capacities compared with ATPC.

Figs. 6 and 7 show achievable capacity by ATPC and LBT when CRS stations are located indoor sites. The results show indoor cases dramatically increases the capacities compared with the outdoor cases. When we focus on the cell fringe of the MCS, indoor CRS-BSs with ATPC attains about 3 times capacities of outdoor case, as for LBT case more than 20 times capacity of the outdoor case are obtained in indoor case. The differences come from penetration losses by building walls, so we have to note that the difference largely depends on

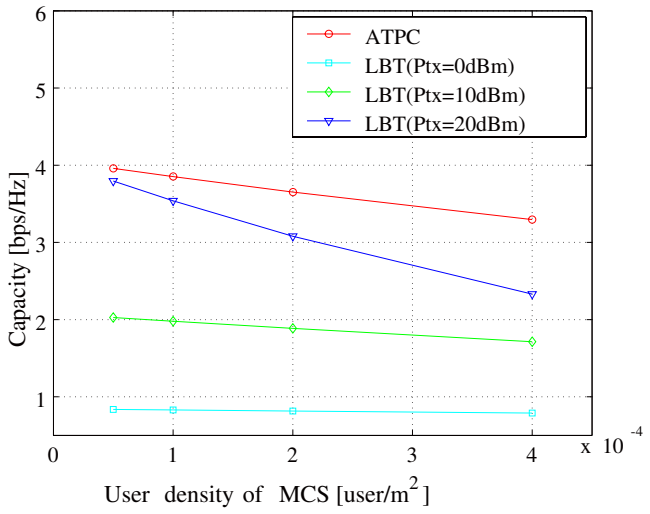

Fig. 8. Area-averaged cell capacities achieved by the CRS versus the effective user density of the MCS MS, indoor

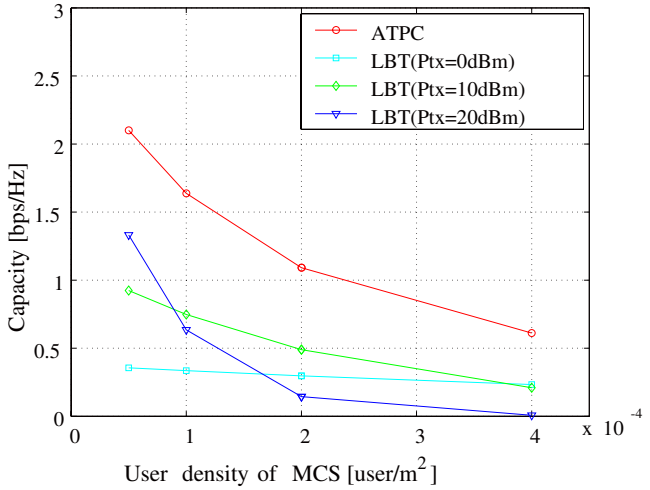

Fig. 9. Area-averaged cell capacities achieved by the CRS versus the effective user density of the MCS MS, outdoor

the assumed value of the loss. Moreover, if we compare the capacities of ATPC an LBT, ATPC attains about 1.5 times capacity of LBT in the indoor cases and 10 times the capacity in the outdoor cases. As for the outdoor case with LBT, $P_{tx,crs}$ of 10dBm in LBT cases is far from optimal, which is shown below.

Fig. 8 shows the area-averaged cell capacities achieved by the CRS versus the effective user densities of the MCS MSs $\rho_{mcs,ms}$, when CRS stations are located at indoor sites. The results show that ATPC offers higher capacity than LBT for all $\rho_{mcs,ms}$s. It is also observed that CRSs especially with ATPC achieves spectrum usage efficiency even though existence of MCS restrict the transmit opportunities of CRSs.

Fig. 9 shows the average cell capacities achieved by the CRS, when CRS stations are located at outdoor sites. The results show CRS capacities of ATPC and LBTs decrease as the density of MCS MS goes high and the gradient is steep compared with the indoor cases. It is because the penetrations losses ease interferences between the two systems. The results implies that CRS capability largely depends on the deployment scenario of the CRS stations.

V. Conclusion

We show a theoretical analysis of achievable capacities by a CRS, when the CRS uses a spectrum allocated to an MCS. Numerical results are also given for several scenarios, where LBT and ATPC are assumed as the sharing mechanisms. Moreover, outdoor and indoor installation of CRS stations are considered. The results show that the ATPC achieves heigher capacity than LBT, and CRSs capacity of outdoor scenario decrease steeply as the density of MCS MS goes high, while the gradient is gentler in indoor scenario. From the geographical distributions of CRS capacities, it is confirmed that CRS capacities at the vicinity of MCS BSs becomes quite a small.

Acknowledgement

This work was supported by the Ministry of Internal Affairs and Communications of Japan under the grant “Research and development of radio resource control technologies among multiple radio systems on the same frequency band”.

References

[1] 3GPP, TR 25.814 ”Physical Layer Aspects for Evolved UTRA,” Jan, 2006
[2] Report ITU-R M.2134, ”Requirement related to technical performance for IMT-Advanced radio interface(s)”, Nov. 2008
[3] FCC, “Facilitating Opportunities for Flexible, efficient and Reliable Spectrum Use Employing Cognitive Radio Technologies,” Report and Order FCC-05-57A1, March 2005
[4] I. J. Mitola *et al.*, “Cognitive radio: making software radios more personal,” *IEEE Personal Commun.,* vol. 6, no. 4, pp.13-18, Aug. 1999
[5] S. Haykin, “Cognitive radio: brain empowered wireless communications,” *IEEE J. Select. Areas Commun.*, vol. 23, no. 2, pp.210-220, Feb. 2005
[6] H. Fujii and H. Yoshino, ”Spectrum Sharing by Adaptive Transmit Power Control for Low Priority Systems and Achievable Capacity,” IEICE Trans. on Commun., vol. E92-B, no. 8, pp.2588-2576, Aug. 2009
[7] S. Stotas *et al.* “Overcoming the Sensing-Throughput Tradeoff in Cognitive Radio Networks,” *in Proc of* IEEE International Conference on Communications (ICC), May 2010
[8] R. Muta *et al.* “Throughput Analysis for Cooperative Sensing in Cognitive Radio Networks,” *in Proc of* IEEE International Symposium on Personal, Indoor and Mobile Radio Communications, Sep. 2009
[9] COST Action 231, ”Digital mobile radio towards future generation systems, Final Report,” European Commission, 1999
[10] Report ITU-R M. 2135 ”Guidelines for evaluation of radio interface technologies for IMT-Advanced”, Dec. 2009